Polarized zone-center phonon modes of wurtzite GaAs

Shanna Crankshaw, Linus C. Chuang, Michael Moewe, and Connie Chang-Hasnain
Applied Science & Technology Group and Department of Electrical Engineering and Computer Sciences, University of California, Berkeley, California 94720, USA

(Received 10 March 2010; revised manuscript received 10 May 2010; published 17 June 2010)

Zone-center optical phonons are studied via polarized micro-Raman scattering in wurtzite GaAs crystals grown on sapphire. Polarized spectra reveal the A_1-E_1 splitting in the Raman spectra of all polar optical modes of the wurtzite crystal. The polar mode splitting can be used to estimate a material birefringence of $\Delta n \sim 0.02$.

DOI: 10.1103/PhysRevB.81.233303 PACS number(s): 63.20.−e

Driven by the substantial interest in producing technologies based on semiconductor structures with reduced dimensionality, researchers in recent years have dedicated significant effort to synthesizing semiconductor nanowires with a variety of growth methods.[1–3] From a materials perspective, one intriguing aspect of nanowire growth is the stability of a wurtzite crystalline phase of standard III-V semiconductors such as InP and GaAs, which in their planar forms always adopt a zincblende crystal structure. This dual stability results in the unanticipated challenge of producing single crystals during the growth process, as well as in necessitating characterization of these new forms of otherwise well-known semiconductors. While wurtzite-zincblende polytypism is known for III-nitride semiconductors,[4] among the III-arsenides and III-phosphides it is unique to the nanoscale under ambient temperature and pressure conditions.[5] For understanding exhibited linear and nonlinear optical properties, modeling behavior, or designing devices upon the nanostructures in which the wurtzite modification appears, its bulk material characterization is of both fundamental and applied interest. We recently reported GaAs needles grown on silicon displaying tips sharp to a few-atom level of ~2–5 nm,[6,7] from which transmission electron microscope (TEM) analysis indicates a wurtzite crystalline structure entirely without twinned zincblende sections. Here, we focus on the vibrational properties of wurtzite GaAs, of especial interest for the very fundamental relationship of Raman scattering efficiencies to electro-optic and nonlinear coefficients of the material.[8,9]

The atomic stacking sequence along the [111] direction of a zincblende crystal (staggered ABCABC) compared to the [0001] direction of the wurtzite crystal (eclipsed ABAB) results in the former being cubic (isotropic), while the latter is hexagonal (anisotropic) with characteristic c-axis and a-axes. The crystalline anisotropy necessitates a careful consideration of polarization dependences in experimental geometries with respect to the wurtzite optical axis (i.e., the c axis). The L(ZB)→Γ(WZ) Brillouin zone-folding relationship[10] of the zincblende [111] to the wurtzite [0001] implies additional phonon modes at the center of the wurtzite Brillouin zone, which could also be expected simply considering the additional atoms present in the four-atom wurtzite primitive cell compared to the two atoms of the zincblende.[11] In order to elucidate the character of individual wurtzite phonon modes, here we concentrate on first-order Raman scattering, which by momentum considerations probes only processes occurring nearly at the center of the Brillouin zone. Wurtzite phonons are classified in their group notation as $\Gamma = 2A_1 + 2B + 2E_1 + 2E_2$, with the A and B modes having atomic displacements parallel to the c axis and the E modes having atomic displacements perpendicular to it. The A_1 and E_1 modes are both Raman and infrared active,[11,12] and as such further split into longitudinal optical (LO) and transverse optical (TO) phonons. These polar modes of the wurtzite crystal, thus, exhibit both an LO-TO and an A_1-E_1 splitting, with the latter resulting from the short-range anisotropy of the force constants. The character of each mode is determined by the form of the associated Raman tensor, which in turn should determine the scattering geometry in which a mode is experimentally observable.[11–15]

Briefly, the wurtzite GaAs samples[6] under investigation are grown by a catalyst-free metal-organic chemical vapor deposition process, which results in uniformly tapered structures with a hexagonal cross-section, as pictured in the scanning electron microscope image in Fig. 1(a). The 180-min growth time of the GaAs needles on sapphire results in a base dimension of ~1.4 μm and length of ~10 μm. The few-nm tips of the crystals permit high-resolution TEM im-

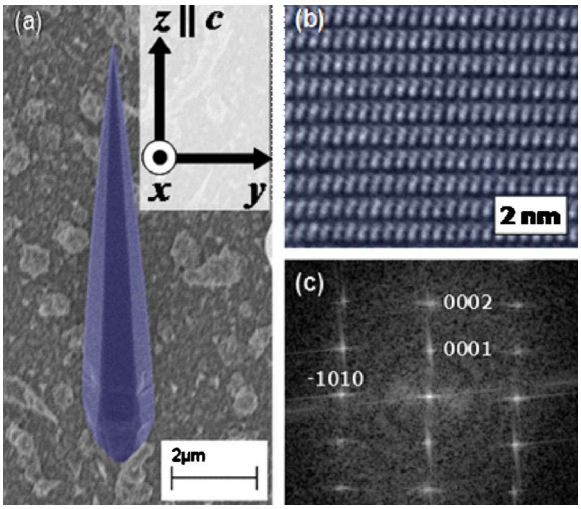

FIG. 1. (Color online) (a) SEM image of a wurtzite GaAs needle tilted from the substrate normal. Length is ~10 μm. (b) HRTEM image near the needle tip and (c) Fourier transform pattern revealing c- and a-axis lattice spacings of 6.524 and 4.031 Å, respectively.

aging, as shown in Fig. 1(b), without any sample-thinning preparation procedure, revealing the growth direction of the needle as always along the wurtzite c axis. Diffraction patterns as in Fig. 1(c) yield a c-axis lattice spacing of 6.524 Å and a-axis spacing of 4.031 Å, for a c/a ratio of 1.618. The taper half-angle, i.e., from the c axis to a vertex of the hexagonal cross-section, is determined from TEM images to be $\sim 4°$.

Micro-Raman scattering is performed on single GaAs needles as pictured in Fig. 1(a) that have been mechanically transferred onto a separate sapphire dummy substrate. The micro-Raman measurements are performed in a backscattering geometry, adapted from a micro-photoluminescence (μ-PL) setup with the use of sharp optical filters (Semrock) in both the excitation and collection paths. The excitation source is a home-built tunable single-mode Ti:Sapphire ring laser which passes through an angle-tunable short-pass filter, half wave plate, polarizer, and beamsplitter before being focused to a ~ 2 μm spot by a 20x, 0.4 numerical aperture objective lens (Mitutoyo). The spot is focused near the base of the needle so as to maximize the sample volume probed and therefore also the signal strength. The scattered light passes through the same beamsplitter, long-pass filter, and polarizer before being focused into a single-stage f =0.75 m spectrometer, dispersed by a 900 g/mm holographic grating, and collected with a nitrogen-cooled silicon charge-coupled detector, for a final spectral resolution of ~ 0.4 cm^{-1} per pixel for the near-infrared (NIR) wavelengths used here.

The backscattering geometry of the measurement means that the direction of the incident light $\boldsymbol{k}_i$ is antiparallel to the collected scattered light, $\boldsymbol{k}_s = -\boldsymbol{k}_i$. As the dispensed needles lie flat on one of their hexagonal faces, the $\pm\boldsymbol{k}_{i,s}$ directions are approximately perpendicular ($\pm 4°$) to the wurtzite c axis. Defining the c axis as the z-polarization direction as indicated in the inset of Fig. 1(a), the polarization configuration can be specified in the standard Raman shorthand notation as $\boldsymbol{k}_i(\boldsymbol{e}_i\boldsymbol{e}_s)\boldsymbol{k}_s$ where $\boldsymbol{e}_i$ and $\boldsymbol{e}_s$ represent the polarization of the incident and scattered light, respectively, as $-x(zz)x$, $-x(zy)x$, $-x(yz)x$, or $-x(yy)x$. In principle, these configurations correspond to the observable scattering lines governed by the form of the Raman tensor for a particular mode, although for these GaAs needles they are only nominal designations because of the near-band-gap excitation and the refraction of light into the tapered structure creating a mixture of angles exciting additional modes in the material.

The NIR excitation represents Raman scattering approaching a resonant regime for the LO phonon, where its strong Fröhlich interaction results in up to three LO overtones present in the room-temperature needle (290 K) spectra. Here we focus on only the first-order processes, as depicted in Fig. 2 for an excitation wavelength of 825.0 nm. This choice of excitation strongly enhances scattering by the LO phonon, but is still far from the expected outgoing resonance condition itself.[16,17] While in general the TO (LO) phonon is backscattering-forbidden from {100} ({110}) zincblende surfaces, it is allowed from {110} ({100}) ones, so that the choice of a cleaved {110} surface of an undoped zincblende [001] epilayer reference sample grown by molecular beam epitaxy makes the TO phonon visible by the usual selection rules[14] and the otherwise-forbidden LO one strongly visible because of the resonance (band gap) proximity.[16] The background resulting from the sample PL has been subtracted from all of the spectra in Fig. 2 as a simple linear function over the small range of wave numbers of interest. The zincblende reference yields TO and LO lines at 268.6 full width at half maximum (FWHM) 5.8 cm^{-1} and 292.1 cm^{-1} (FWHM 4.5 cm^{-1}), respectively, and from a freshly cleaved surface of the epilayer also a surface-optical (SO) phonon[14] at 280.5 cm^{-1} (FWHM 7.2 cm^{-1}) which becomes an indistinct low-energy shoulder of the LO phonon upon further exposure to air. Thus, the zincblende GaAs spectrum, whose raw data in Fig. 2 are shown as gray squares, may be represented very well by a sum of three Lorentzians (solid black line in the scattering spectrum), for the TO, SO, and LO lines.

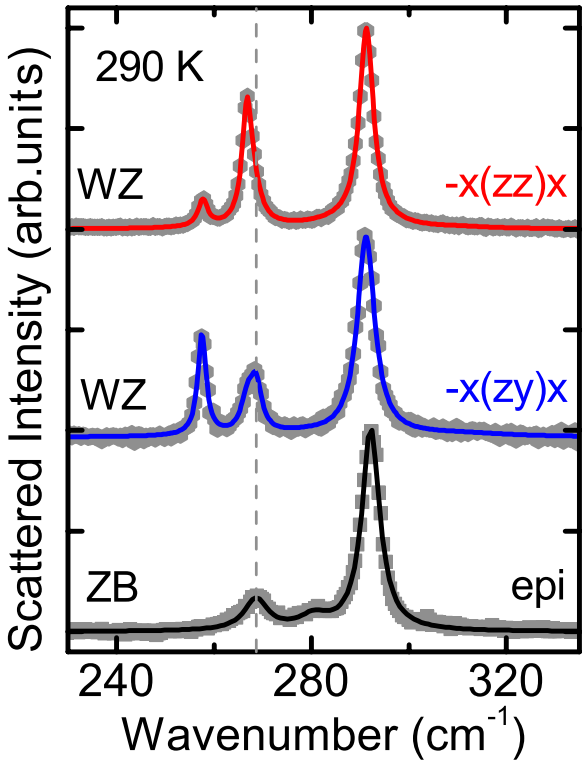

FIG. 2. (Color online) Backscattering spectra of a zincblende (ZB) GaAs epilayer and wurtzite (WZ) GaAs needles at 290 K, each normalized to the intensity of its LO line and offset for clarity. Gray dots represent raw data, solid lines multi-Lorentzian fits. The freshly-cleaved ZB epilayer has a distinct SO phonon at 280 cm^{-1} in addition to its LO mode at 292.1 cm^{-1} and TO mode (indicated by the vertical dashed line) at 268.6 cm^{-1}. An SO contribution is also used to fit the polarized $-x(zy)x$ and $-x(zz)x$ wurtzite spectra, which show a mode at 257.5 cm^{-1} attributable to a WZ E_2^{high} mode.

Figure 2 also shows scattering spectra of the wurtzite GaAs needles recorded in two different polarization configurations, modifying the relative intensities of the observed lines. Each spectrum is normalized to the intensity of its own LO phonon and offset for clarity. The solid lines in the $-x(zy)x$ and $-x(zz)x$ wurtzite spectra are again multi-Lorentzian fits to the raw data represented by gray hexagons, including an unresolved SO phonon necessary to reproduce

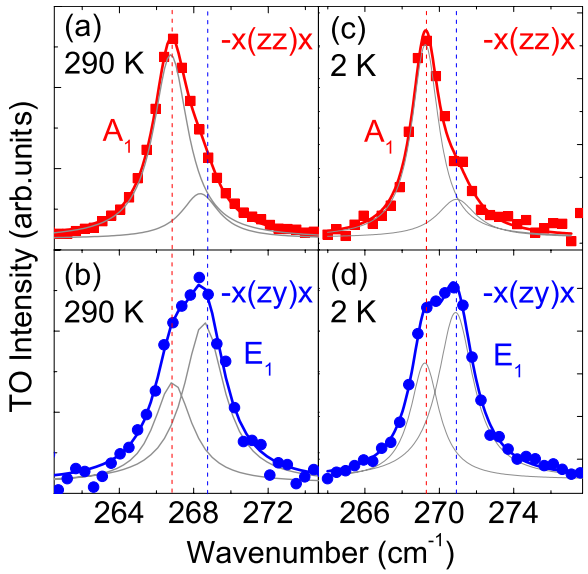

FIG. 3. (Color online) TO phonon measured in $-x(zz)x$ (red squares) and $-x(zy)x$ (blue circles) geometries, corresponding to A_1 and E_1 configurations, respectively. A two-component fit (gray lines) of the (a) 290 K A_1 spectrum and (b) 290 K E_1 spectrum yields identical values for the Raman shifts of 268.6 cm^{-1} (A_1) and 266.8 cm^{-1} (E_1), each with FWHM ~2.5 cm^{-1}. The (c) A_1 and (d) E_1 spectra at 2 K are slightly better resolved due to the FWHM decrease to 1.8 cm^{-1}, again yielding consistent shifts of 269.2 cm^{-1} (A_1) and 270.9 cm^{-1} (E_1).

the spectra but far less prominent than in nanowire samples.[18] The wurtzite LO phonon is usually observed at 291.3 cm^{-1} (FWHM 4.0 cm^{-1}), similar in energy and even narrower in linewidth than that of the zincblende GaAs spectrum, testifying to the crystalline quality and single phase of the needle here. Compared to the epilayer, both of the wurtzite GaAs spectra clearly display an additional lower-energy mode at 257.5 cm^{-1} (FWHM 2.0 cm^{-1}). A mode at this energy was recently observed in GaAs nanowires exhibiting zincblende-wurtzite twinning,[19] which had a substantially smaller sample volume than that probed here. Given the wurtzite phase of the samples here and considering the crystallographic L(ZB)→Γ(WZ) mapping, we can unambiguously attribute this mode to the nonpolar E_2^{high} optical phonon of the wurtzite structure. For the TO scattering around 268 cm^{-1}, however, a more careful examination of the polarization behavior is necessary for mode assignments, as described below.

The 290 K wurtzite TO spectrum collected in the $-x(zz)x$ (nominally A_1) configuration displays an asymmetric lineshape, as shown in detail in Fig. 3(a). This peak can be represented very well by a sum of two Lorentzians, shown as gray lines in Fig. 3(a), although this must be physically motivated since asymmetric line broadening can also be indicative of anharmonic decay processes.[13] A two-component fit indeed has a very clear meaning for the wurtzite GaAs here: incomplete polarization suppression of the distinct A_1(TO) and E_1(TO) modes of the anisotropic crystal. This is ascertained by comparing the nominally A_1(TO) spectrum collected in the $-x(zz)x$ geometry to the nominally E_1(TO) one collected in an $-x(zy)x$ configuration, shown similarly in Fig. 3(b). Both of these can be fit by two Lorentzians, and—crucially—in doing so one obtains the same energies for each component of the $-x(zz)x$ and $-x(zy)x$ fits, indicated by the vertical lines in Fig. 3. In other words, the apparent asymmetry of the TO line results from the simultaneous appearance of both polar modes, likely because of the angular mixture implicit for the tapered structure. The acquisition of polarized spectra nonetheless reveals consistent results yielding phonon energies of A_1(TO)=266.8 cm^{-1} and E_1(TO) =268.6 cm^{-1}. This 1.8 cm^{-1} polarization splitting is comparable to the linewidth of the modes themselves, each with a FWHM of ~2.5 cm^{-1} at 290 K. Cooling the sample to 2 K narrows the linewidths to ~1.8 cm^{-1}—nearly instrument limited—but applying the same two-component fit to both the $-x(zz)x$ and $-x(zy)x$ spectra again yields consistent results, with the 2 K shifts of A_1(TO)=269.2 cm^{-1} and E_1(TO)=270.9 cm^{-1} depicted in Figs. 3(c) and 3(d).

The incomplete A_1-E_1 suppression of the TO mode also suggests an explanation for the slight shift of the LO mode sometimes seen in the $-z(xy)z$ spectra from its usual 290 K value of 291.3 cm^{-1} to 291.7 cm^{-1}. The E_1(LO) mode is forbidden in a backscattering geometry according to the tensor selection rules, and a fitting procedure like that depicted in Fig. 3 is complicated by the presence of an unresolved SO mode on the lower-energy side. While the attribution of A_1(LO)=291.3 cm^{-1} is quite clear, E_1(LO) may only tentatively be specified as 291.7 cm^{-1}, although even in an E_1(LO)-allowed measurement geometry such as right-angle scattering this sub-cm^{-1} separation would prove difficult to resolve. Nonetheless, these A_1(TO), E_1(TO), A_1(LO), and E_1(LO) energies are further supported by a comparison of the *relative* numbers with other binary semiconductor materials. The 290 K absolute splitting of the A_1(TO) and E_1(TO) modes of only 1.8 cm^{-1} is indeed expected given the relatively small energy difference of the LO and TO groups themselves, a manifestation of the strength of the long-range Fröhlich interaction separating the LO modes from the TO ones over the short-range anisotropy of the force constants differentiating A_1 from E_1.[12,20] That the LO-TO splitting is much larger than either the A_1(TO)-E_1(TO) or A_1(LO)-E_1(LO) separation is true for all of the commonly-wurtzite binary semiconductors, such as many II-VI semiconductors and the III-nitrides, as gathered from literature sources.[11–13,21,22] This may be quantified between various hexagonal materials by comparing the quantity $\gamma=(\nu_{E1}-\nu_{A1})/[(\nu_{E1}+\nu_{A1})/2]$—i.e., the A_1-E_1 splitting divided by their average value—for both the TO and LO phonons. The TO polarization contrast, γ_{TO}, is larger than the LO one, γ_{LO}, by a factor ranging from γ_{TO}/γ_{LO} ~3–6, generally scaling with the material's c/a ratio, as depicted in Fig. 4 including the present experimental numbers for GaAs. Hence despite the smallness of the absolute polarization splittings observed, the relative values are very much in line with other binary wurtzite semiconductors.

Lastly, as a practical consequence of having examined polar phonon modes, an estimate of the birefringence of wurtzite GaAs may be obtained from the independent Lydanne-Sachs-Teller relationships[14,20,23] for the $c^{\parallel}$ and $c^{\perp}$ directions: $\varepsilon_0^{\perp}/\varepsilon_\infty^{\perp}=\omega_{E1(LO)}^2/\omega_{E1(TO)}^2$ and $\varepsilon_0^{\parallel}/\varepsilon_\infty^{\parallel}$

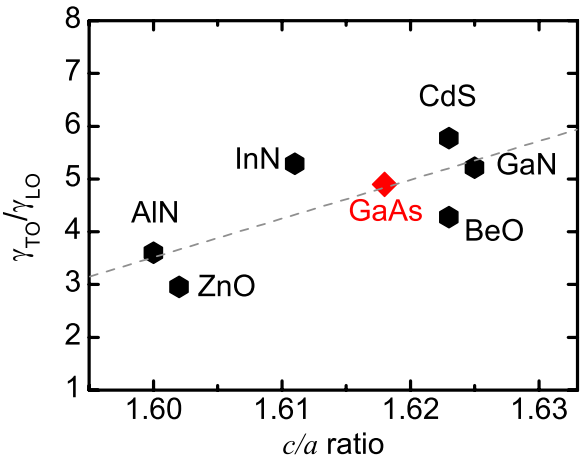

FIG. 4. (Color online) Comparison of the A_1-E_1 polarization splitting γ of the TO phonon with that of the LO phonon for various wurtzite binary semiconductors. Except for GaAs (this study), the structural c/a values are from Ref. 26, and literature values for the phonon energies were collected for AlN (Ref. 21), ZnO (Ref. 13), InN (Ref. 22), BeO (Ref. 12), CdS (Ref. 12), and GaN (Ref. 11).

$=\omega^2_{A1(\mathrm{LO})}/\omega^2_{A1(\mathrm{TO})}$. If we assume that at frequencies much higher than those of the measured phonon vibrations the dielectric constant is isotropic, we can take as ε_∞ the cubic value of 10.9[14] and obtain a static birefringence of $\Delta n = n_e - n_o = 0.019$, where n_e and n_o represent the extraordinary and ordinary indices, respectively. For a real anisotropy, the expected $\varepsilon_\infty^{\parallel} > \varepsilon_\infty^{\perp}$ implies that $\Delta n = 0.019$ represents a minimum value for the birefringence. A more detailed analysis would have to consider the change in the Raman-scattered intensities of the observed modes under the implicit dephasing effects of extraordinary light propagation in a uniaxial medium, rather than only the change in mode frequencies.[24] Nonetheless, any birefringence is of interest because it potentially allows for bulk phase-matching conditions to be reached in nonlinear optical processes,[25] which is not possible for a cubic crystal.

In summary, a polarized first-order Raman study of bulk wurtzite GaAs has clearly revealed the anisotropic nature of the crystal in the zone-center phonon modes, further providing an estimate of the material birefringence. The 290 K wurtzite E_2^{high} phonon occurs at 257.5 cm^{-1}, with the A_1(TO) mode at 266.8 cm^{-1} and E_1(TO) mode at 268.6 cm^{-1} definitively resolved despite the incomplete separation. The A_1(LO) mode at 291.3 cm^{-1} is separated by an even smaller amount from its E_1(LO) counterpart, tentatively specified as 291.7 cm^{-1}, consistent with hexagonal binary semiconductor material trends.

[1] X. Duan and C. M. Lieber, Adv. Mater. **12**, 298 (2000).
[2] L. C. Chuang, M. Moewe, C. Chase, N. P. Kobayashi, C. Chang-Hasnain, and S. Crankshaw, Appl. Phys. Lett. **90**, 043115 (2007).
[3] A. Fontcuberta i Morral, D. Spirkoska, J. Arbiol, M. Heigoldt, J. R. Morante, and G. Abstreiter, Small **4**, 899 (2008).
[4] Chin-Yu Yeh, Z. W. Lu, S. Froyen, and Alex Zunger, Phys. Rev. B **46**, 10086 (1992).
[5] M. I. McMahon and R. J. Nelmes, Phys. Rev. Lett. **95**, 215505 (2005).
[6] M. Moewe, L. C. Chuang, S. Crankshaw, C. Chase, and C. Chang-Hasnain, Appl. Phys. Lett. **93**, 023116 (2008).
[7] M. Moewe, L. C. Chuang, S. Crankshaw, K. W. Ng, and C. Chang-Hasnain, Opt. Express **17**, 7831 (2009).
[8] W. D. Johnston and I. P. Kaminow, Phys. Rev. **188**, 1209 (1969).
[9] I. P. Kaminow, *Introduction to Electrooptic Devices* (Academic Press, Orlando, Florida, 1974).
[10] Chin-Yu Yeh, Z. W. Lu, S. Froyen, and Alex Zunger, Phys. Rev. B **45**, 12130 (1992).
[11] H. Siegle, G. Kaczmarczyk, L. Filippidis, A. P. Litvinchuk, A. Hoffmann, and C. Thomsen, Phys. Rev. B **55**, 7000 (1997).
[12] C. A. Arguello, D. L. Rousseau, and S. P. S. Porto, Phys. Rev. **181**, 1351 (1969).
[13] R. Cusco, E. Alarcon-Llado, L. Artus, J. Ibanez, J. Jimenez, B. Wang, and M. J. Callahan, Phys. Rev. B **75**, 165202 (2007).
[14] P. Yu and M. Cardona, *Fundamentals of Semiconductors* (Springer, New York, 2005).
[15] T. Livneh, J. Zhang, G. Cheng, and M. Moskovits, Phys. Rev. B **74**, 035320 (2006).
[16] R. Trommer and M. Cardona, Phys. Rev. B **17**, 1865 (1978).
[17] M. Brewster, O. Schimek, S. Reich, and S. Gradecak, Phys. Rev. B **80**, 201314(R) (2009).
[18] D. Spirkoska, G. Abstreiter, and A. Fontcuberta i Morral, Nanotechnology **19**, 435704 (2008).
[19] I. Zardo, S. Conesa-Boj, F. Peiro, J. R. Morante, J. Arbiol, E. Uccelli, G. Abstreiter, and A. Fontcuberta i Morral, Phys. Rev. B **80**, 245324 (2009).
[20] R. Loudon, Adv. Phys. **13**, 423 (1964).
[21] L. E. McNeil, M. Grimsditch, and R. H. French, J. Am. Ceram. Soc. **76**, 1132 (1993).
[22] V. Yu. Davydov, V. V. Emtsev, I. N. Goncharuk, A. N. Smirnov, V. D. Petrikov, V. V. Mamutin, V. A. Vekshin, S. V. Ivanov, M. B. Smirnov, and T. Inushima, Appl. Phys. Lett. **75**, 3297 (1999).
[23] R. H. Lyddane, R. G. Sachs, and E. Teller, Phys. Rev. **59**, 673 (1941).
[24] P. Alonso-Gutiérrez, M. L. Sanjuan, and M. C. Moron, Phys. Rev. B **71**, 085205 (2005).
[25] R. Chen, S. Crankshaw, T. Tran, L. C. Chuang, M. Moewe, and C. Chang-Hasnain, Appl. Phys. Lett. **96**, 051110 (2010).
[26] G. A. Jeffrey, G. S. Parry, and R. L. Mozzi, J. Chem. Phys. **25**, 1024 (1956).